Biosensors and Bioelectronics 26 (2010) 504–510

Contents lists available at ScienceDirect

Biosensors and Bioelectronics

journal homepage: www.elsevier.com/locate/bios

Enhanced electrochemical oxygen reduction-based glucose sensing using glucose oxidase on nanodendritic poly[*meso*-tetrakis(2-thienyl)porphyrinato]cobalt(II)-SWNTs composite electrodes

Wei Chen[a,1], Yu Ding[a], Joshua Akhigbe[b], Christian Brückner[b], Chang Ming Li[c], Yu Lei[a,*]

[a] Department of Chemical, Materials and Biomolecular Engineering, University of Connecticut, Storrs, CT 06269-3222, USA
[b] Department of Chemistry, University of Connecticut, Storrs, CT 06269-3060, USA
[c] School of Chemical and Biomedical Engineering, Nanyang Technological University, 637457, Singapore

ARTICLE INFO

Article history:
Received 28 April 2010
Received in revised form 5 July 2010
Accepted 15 July 2010
Available online 7 August 2010

Keywords:
Glucose
Glucose oxidase
Biosensor
Direct electrochemistry
Nanodendritic pCoTTP
SWNTs

ABSTRACT

The direct electrochemistry of glucose oxidase immobilized on a nanodendritic poly[*meso*-tetrakis(2-thienyl)porphyrinato]cobalt(II)-single walled carbon nanotube modified glassy carbon electrode (pCoTTP-SWNTs-Nafion-GOD/GCE) is reported. The immobilized GOD retained its activity and exhibited a surface controlled, reversible two-proton and two-electron transfer reaction with a fast heterogeneous electron transfer rate constant (k_s) of 1.01 s^{-1}. The pCoTTP-SWNTs-Nafion matrix also showed an extremely low peak potential of −0.2 V vs. Ag/AgCl and strong response with respect to oxygen reduction. This forms the basis for the use of the pCoTTP-SWNTs-Nafion-GOD composite as a sensing platform for oxygen reduction-based glucose detection. The apparent Michaelis–Menten constant ($K_{m,app}$) was estimated to be as low as 0.98 mM. A linear range up to 1 mM glucose with a low detection limit of 5.33 μM (S/N = 3) and a high sensitivity of 16.57 μA mM^{-1} cm^{-2} was achieved. The biosensor also shows excellent selectivity against 0.2 mM uric acid and ascorbic acid. These results indicate that the pCoTTP-SWNTs-Nafion-GOD/GCE has potential application in sensitive and selective glucose detection.
Published by Elsevier B.V.

1. Introduction

Glucose oxidase (GOD) is a dimeric protein that catalyzes the oxidation of β-D-glucose to D-glucono-1,5-lactone, which subsequently hydrolyzes non-enzymatically to gluconic acid. Two flavin adenine dinucleotide (FAD) cofactors are tightly bound to and deeply buried in the protein (Hecht et al., 1993). In the GOD-catalyzed glucose oxidation, FAD serves as the initial electron acceptor and is reduced to $FADH_2$. Then $FADH_2$ is oxidized by the final electron acceptor, molecular oxygen (O_2), because it has a higher reduction potential, while O_2 is reduced to hydrogen peroxide. Due to GOD's shielding of the redox active centers by an insulating protein shell, the direct electron transfer between GOD and bare glassy carbon (GCE) or gold electrodes is greatly inhibited. However, a direct electron transfer between FAD and electrode surfaces is desirable for the fundamental study of the electron transfer processes and the realization of electrochemical glucose sensors (Courjean et al., 2009; Demin and Hall, 2009; Liu et al., 2004, 2007b). Thus, in order to facilitate the direct electron transfer process between GOD and electrode surfaces, various materials such as carbon nanotubes (CNTs) and nanoparticles have been utilized (Demin and Hall, 2009; Ivnitski et al., 2008; Liu et al., 2007a; Patolsky et al., 2004; Xiao et al., 2003).

Particularly CNTs gained attention in electrocatalysis and biosensing applications owing to their high electrical conductivity, high surface to volume ratio, and good chemical and mechanical stability (Azamian et al., 2002; Britto et al., 1996; Lin et al., 2004; Musameh et al., 2002; Yu et al., 2003b). A number of glucose sensors based on CNTs modified electrodes were developed (Cai and Chen, 2004; Lin et al., 2004; Liu et al., 2005b; Luo et al., 2006; Luong et al., 2004; Wang et al., 2003). These reports have shown that CNTs, either single- (SWNTs) or multi-walled CNTs (MWCNTs) can provide direct electron transfer channels between the active centers of GOD and the electrode. In addition, CNTs also provide a suitable matrix for GOD immobilization.

GOD-based glucose sensing can be accomplished either by directly measuring the electrons released by GOD, or indirectly by

* Corresponding author at: Department of Chemical, Materials and Biomolecular Engineering, University of Connecticut, 191 Auditorium Rd, Storrs, CT 06269-3222, United States. Tel.: +1 860 486 4554; fax: +1 860 486 2959.
E-mail address: ylei@engr.uconn.edu (Y. Lei).
[1] Current address: School of Life Science and Technology, Huazhong University of Science and Technology, 1037 Luoyu Road, Wuhan 430074, China.

0956-5663/$ – see front matter. Published by Elsevier B.V.
doi:10.1016/j.bios.2010.07.062

oxidation of the hydrogen peroxide formed. One other indirect process measures oxygen reduction due to the consumption of oxygen by GOD in the presence of glucose. However, this method requires a low potential oxygen reduction electrode to minimize the interferences inherent when applying higher potentials. Thus, a number of electrocatalytic oxygen reduction electrodes have been developed to allow the realization of oxygen reduction-based glucose biosensors. For example, celestine blue allows the amperometric oxygen reduction at a low applied potential of −0.35 V vs. Ag/AgCl (Noorbakhsh et al., 2008), but it is water soluble and catalyst leakage problem occurs. An osmium (Os) complex with CNTs allows an improved amperometric oxygen reduction at −0.25 V vs. Ag/AgCl. However, Os is expensive and desorption of the metal complex is observed (Salimi et al., 2009).

We recently reported a novel and inexpensive poly[*meso*-tetrakis(2-thienyl)porphyrinato]cobalt(II) (pCoTTP)-modified electrode that effectively lowered the overpotential for oxygen reduction peak to −0.2 V vs. Ag/AgCl. The pCoTTP-modified glassy carbon electrode (GCE) displayed no stability or leakage problems in organic or aqueous solutions, thus providing an overall excellent electrocatalyst for oxygen reduction (Chen et al., 2010).

Here we report a new electrode coating that combines the advantages of nanodendritic pCoTTP, SWNTs, and GOD, which is suitable for glucose sensing (Supplemental Fig. 1). The direct electrochemistry of GOD on the pCoTTP-SWNTs-modified electrode was investigated using cyclic voltammetry. Further, the sensitive and selective amperometric oxygen reduction-based glucose detection was achieved using this pCoTTP-SWNTs-Nafion-GOD-modified GCE. The kinetic parameters of immobilized GOD were also calculated and compared to literature values.

2. Experimental

2.1. Chemicals

GOD (129,900 units/g), Nafion (20 wt% in ethanol), 0.01 M phosphate buffer saline (PBS, pH = 7.4), acetone, and tetrabutylammonium hexafluorophosphate ($TBAPF_6$) were purchased from Sigma–Aldrich. The pH of PBS was adjusted using 1.0 M NaOH or 0.5 M H_2SO_4, respectively. β-D-Glucose and dichloromethane (CH_2Cl_2) were obtained from Acros. CoTTP was prepared as previously described (Chen et al., 2010). Ascorbic acid (AA) and uric acid (UA) were purchased from Fisher Scientific. SWNTs (purity > 90 wt%, outer diameter of 1–2 nm, length of 5–30 μm) were bought from Cheap Tubes Inc., (Vermont, USA) and used as received. All solutions used in the experiments were prepared with deionized water (18.2 MΩ cm, EASYpure, Barnstead, USA). All β-D-glucose solutions used were allowed to achieve mutarotation equilibrium for at least 24 h before use. To de-aerate the solutions, the solutions were purged with high purity nitrogen gas (99.99%, Airgas) for 15 min. A nitrogen atmosphere was maintained over the solution during the anaerobic electrochemical measurements.

2.2. Apparatus

All electrochemical measurements were carried out using a conventional three-electrode system including a bare or modified glassy carbon working electrode (GCE, 3 mm diameter), an Ag/AgCl sat. KCl reference electrode, and a platinum wire counter electrode. A computer-controlled VMP3 electrochemical workstation was used for all electrochemical studies. A JEOL 6335F field emission scanning electron microscope (FESEM) was employed to investigate the morphology of the electrode surfaces.

2.3. Electropolymerization of nanodendritic pCoTTP

Prior to electrochemical polymerization, the GCE was successively polished with 1.0, 0.3, and 0.05 μm α-Al_2O_3 powders and sonicated in a water-bath for about 5 min after each polishing step. Then the electrode was rinsed thoroughly in deionized water before use. The electrode was allowed to air-dry and was then placed into a dichloromethane solution containing 1 mM CoTTP monomer and 0.1 M $TBAPF_6$ as supporting electrolyte. Repetitive cycling from 0 to 2 V vs. Ag/AgCl wire was carried out to deposit the pCoTTP film on the surface of the GCE. The modified electrode was then rinsed with acetone to remove any residual CoTTP (or soluble oligomers), and air-dried.

2.4. Fabrication of pCoTTP-SWNTs-Nafion-GOD/GCE

20 mg SWNTs were dispersed in 1 mL of 1 wt% Nafion solution (in ethanol) under sonication for 30 min. GOD (50 mg/mL in 0.01 M PBS) was then added into the SWNTs-Nafion dispersion at a 1:1 (v/v) ratio to prepare the mixture consisting of 10 mg/mL SWNTs, 0.5 wt% Nafion and 25 mg/mL GOD in 0.01 M pH 7.4 PBS buffer. After further 10 min sonication, a 5 μL aliquot of the mixture was dropped onto the pCoTTP-modified GCE, and the electrode was air-dried at room temperature for 1 h. The modified electrode was kept in 0.01 M pH 7.4 PBS buffer before each electrochemical measurement. In addition, the pCoTTP-SWNTs-Nafion/GCE, drop-deposited Nafion/GCE, Nafion-GOD/GCE, and SWNTs-Nafion-GOD/GCE were prepared as control electrodes.

2.5. Electrochemical measurements of glucose

Cyclic voltammetric measurements were performed using an electrochemical workstation (Bio-logic SA VMP3) in a conventional three-electrode configuration, including a working electrode, an Ag/AgCl reference electrode, and a platinum counter electrode. Glucose measurements were carried out in 0.01 M pH 7.4 PBS buffer at room temperature. For the amperometric glucose detection, all measurements were performed by applying a potential of −0.2 V vs. Ag/AgCl to the working electrode and allowing the transient background current to decay to a steady-state value, prior to the addition of glucose. The current response due to the addition of glucose was recorded. The solution was mechanically stirred (magnetic stirring with Teflon-coated stirr bar) to provide convective transport.

3. Results and discussion

3.1. Characterization of nanodendritic pCoTTP, SWNTs-Nafion and SWNTs-Nafion-GOD films

The morphologies of electrodeposited pCoTTP, drop-cast SWNTs-Nafion and SWNTs-Nafion-GOD films on the GCE were investigated using SEM. As shown in Fig. 1A, electrodeposited pCoTTP forms an interlaced nanodendritic structure. The enlarged surface area and channels are beneficial for increased electron transfer and oxygen reduction. The drop-cast SWNTs-Nafion composite exhibits a porous structure, likely consisting of numerous stacked bundles of SWNTs embedded in the polymer matrix (Fig. 1B). Such porous structure could provide a large surface area for GOD loading and providing large GOD–electrode interfaces while the SWNTs bundles can offer effective electron-conducting pathways. In contrast, the SWNTs-Nafion-GOD film shows a smooth surface (Fig. 1C), indicating the incorporation of GOD into the porous SWNTs-Nafion composite. After casting the SWNTs-Nafion-GOD mixture onto a pCoTTP-modified GCE (pCoTTP-SWNTs-Nafion-GOD/GCE), the close contact was achieved between the pCoTTP, the enzyme, and the SWNTs. SWNTs and

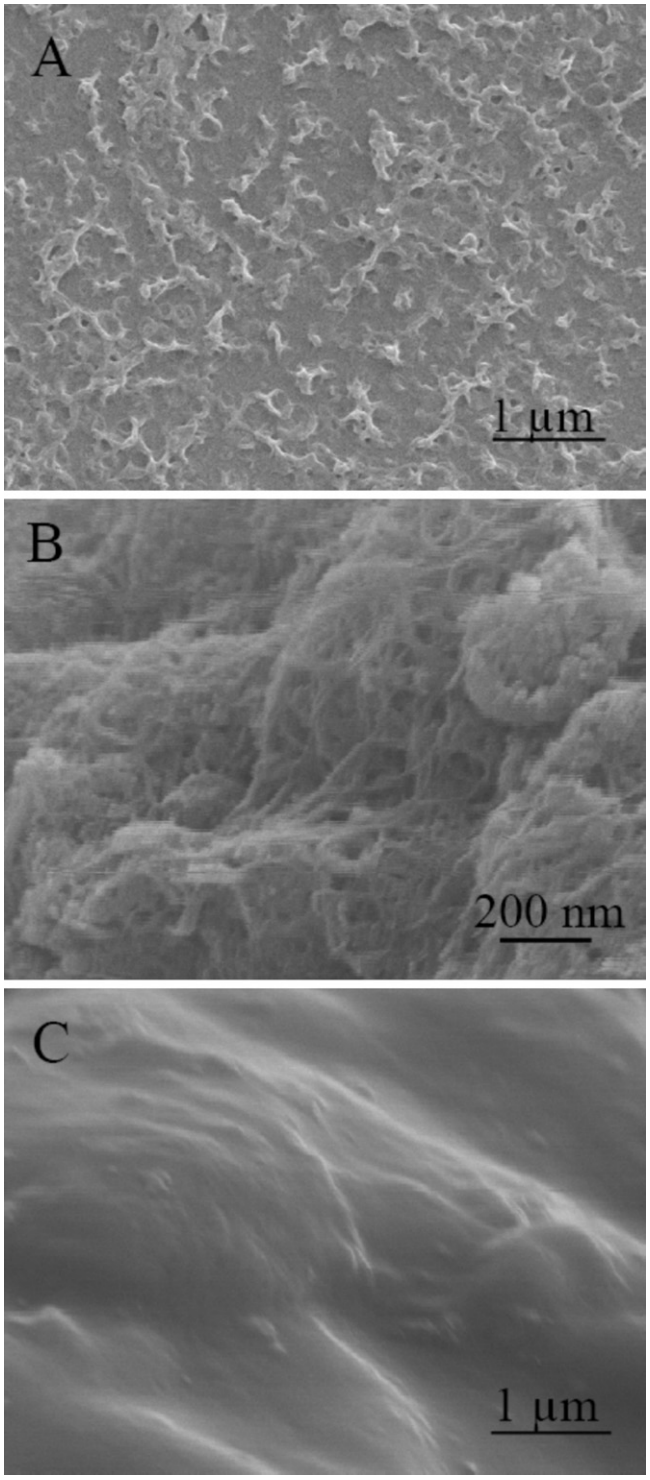

Fig. 1. (A) SEM images of pCoTTP-, (B) SWNTs-Nafion-, and (C) SWNTs-Nafion-GOD-modified surfaces.

pCoTTP together can further reduce the insulating property of proteins and facilitate direct electron transfer between electrode and GOD.

3.2. Direct electrochemistry of GOD

The electrochemistry of the immobilized GOD was tested using cyclic voltammetry in anaerobic 0.01 M pH 7.4 PBS buffer solutions at a scan rate of 50 mV/s. Fig. 2 presents the CVs of GCEs modified with a variety of films. A simple Nafion-coated GCE is not electrochemically active (Fig. 2A, trace a). Incorporation of GOD into this film (Nafion-GOD/GCE) results in the expression of a pair of barely visible redox signals (Fig. 2A, trace b). After the incorporation of SWNTs into the matrix (SWNTs-Nafion-GOD/GCE), an enhanced current signal and a pair of well defined redox peaks with an anodic peak potential at −0.426 V and a cathodic peak potential at −0.489 V can be detected (Fig. 2A, trace c). The formal potential ($E^{0'}$) calculated by averaging the anodic and cathodic peak potentials is −0.462 V, with a peak potential separation of about 72 mV, suggestive of a quasi-reversible process (Bard and Faulkner, 2001). The redox peaks are assigned to the direct electrochemistry of GOD, which is the characteristic of reversible electron transfer process between the electroactive center, FAD, and the electrode. The reaction can be schematically expressed as follows: GOD-FAD + $2H^+ + 2e^- \leftrightarrow$ GOD-$FADH_2$ (Bao et al., 2008). We attribute the enhanced current signal in the presence of the SWNTs to the large GOD-SWNT interface area and good conductivity of the SWNTs, forming many efficient paths for direct electron conduction in and out of the enzyme.

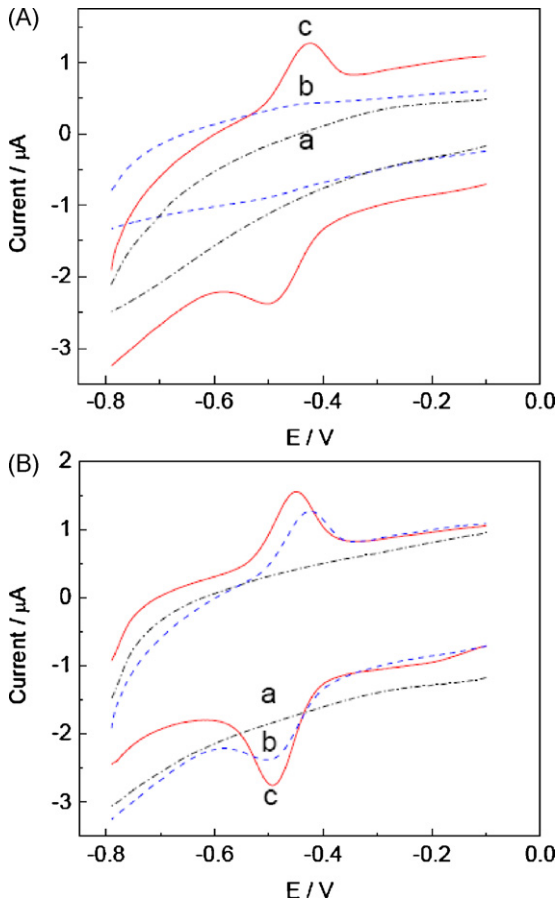

Fig. 2. (A) CVs of Nafion/GCE (a), Nafion-GOD/GCE (b) and SWNTs-Nafion-GOD/GCE (c). (B) CVs of pCoTTP-SWNTs-Nafion/GCE (a), SWNTs-Nafion-GOD/GCE (b) and pCoTTP-SWNTs-Nafion-GOD/GCE (c) in N_2-saturated 0.01 M pH 7.4 PBS buffer at a scan rate of 50 mV/s.

The effect of the pCoTTP-modified electrode surface on the direct electrochemistry of GOD (pCoTTP-SWNTs-Nafion-GOD/GCE) is shown in Fig. 2B, trace c. One can see that the anodic and cathodic peak potentials of GOD are shifted to −0.451 V and −0.493 V, respectively. The formal redox potential ($E^{0'}$) is −0.472 V and the peak potential separation is 42 mV. The peak potential separation is significantly smaller than that observed in the absence of the nano-dendritic pCoTTP (72 mV; Fig. 2B, trace b). In addition, the redox

peaks obtained at the pCoTTP-SWNTs-Nafion-GOD/GCE are sharper and the peak currents are higher. The reduced peak potential separation suggests that a faster and more reversible direct electron transfer was achieved between GOD and the electrode (Bard and Faulkner, 2001). The higher currents also highlight the contribution of the pCoTTP layer. The rough surface evidently provides a better immobilization environment for SWNTs-Nafion-GOD by providing an enlarged conducting surface area with an enhanced electron transfer property between GOD and the electrode. As a comparison, the pCoTTP-SWNTs-Nafion/GCE was used as a control electrode and shows no redox peaks at all due to the lack of GOD (Fig. 2B, trace a).

In order to determine the kinetic parameters of GOD at the pCoTTP-SWNTs-Nafion-GOD-modified electrode, the effect of scan rate on the CV was investigated. The CV scan rates were varied from 10 mV/s to 300 mV/s (Fig. 3A). Both the reduction and oxidation peak currents increase linearly with the scan rate, showing a typical surface controlled quasi-reversible electrochemical behavior (Fig. 3B). These results fit the equation for a Nernstian adsorbate layer ($i_p = n^2F^2\nu A\Gamma^*/RT$), where i_p is the peak current, n is the number of electrons transferred, F is the Faraday constant, R is the gas constant, T is the absolute temperature, ν is the scan rate, A is the electrode area and Γ^* is the surface concentration of electroactive species (Bard and Faulkner, 2001; Ding et al., 2010). According to this equation, the electroactive GOD concentration on the pCoTTP-SWNTs-Nafion-GOD/GCE is 1.12×10^{-10} mol/cm^2, which is nearly two orders of magnitude higher than 2.86×10^{-12} mol/cm^2 determined for GOD entrapped in Nafion on a bare GCE (Zhang et al., 2007). The result indicates the effectiveness of the nanodendritic pCoTTP-SWNT composite with respect to mediating the electron transfer from GOD to the electrode.

As presented in the inset of Fig. 3B, the oxidation peak shifts to more positive potential, while the reduction peak shifts to more negative potential with the increase of scan rates. The anodic and cathodic peak potentials show a linear relationship with the logarithm of scan rates at high scan rate over 100 mV/s, with slopes of $-2.3RT/\alpha nF$ and $2.3RT/(1-\alpha)nF$ for the cathodic peak and anodic peak, respectively. From this, α can be estimated to be 0.298. Knowing α, Laviron theory (Laviron, 1979) allows the electron transfer rate constant (k_s) to be determined according to following equation $\log k_s = \alpha \ln(1-\alpha) + (1-\alpha)\ln\alpha - \log(2.3RT/nF\nu) - \alpha(1-\alpha)(nF\Delta E_p/2.3RT)$, where ΔE_p is the peak potential separation. The k_s value of 1.01 s^{-1} thus determined for the pCoTTP-SWNTs-Nafion-GOD-modified GCE is significantly better than of the value of 0.3 s^{-1} obtained for GOD at aligned SWNT arrays on a modified gold electrode (Liu et al., 2005a) or 0.026 s^{-1} obtained by GOD attached to a self-assembled monolayer of 3,3′-dithiobissulfocinnimidylpropionate (DTSSP) modified gold electrode (Jiang et al., 1995). Our k_s value is also in the same range compared to the value obtained for GOD immobilized on a colloidal gold nanoparticles-Nafion modified GCE (1.3 s^{-1}) (Zhao et al., 2006), for GOD on boron-doped CNT-modified GCE (1.56 s^{-1}) (Deng et al., 2008), and for GOD on a CNTs-Nafion-modified GCE (1.53 ± 0.45 s^{-1}) (Cai and Chen, 2004).

As shown in the above reaction formula, the interconversion of the FAD/FADH$_2$ redox couple involves two electrons and two protons. Thus, the pH value of the solution predictably affects the electrochemical behavior of GOD. Fig. 3C shows the pH-dependent GOD redox peak potential shift in the range from pH 4.0 to pH 10.0 (in N$_2$-saturated, deoxygenated 0.01 M PBS). For each pH value, $E^{0'}$ of the redox couple is calculated and plotted against pH. As shown in the inset of Fig. 3C, $E^{0'}$ changes linearly with the pH with a slope of −56 mV/pH ($R = 0.9991$). This slope is, as expected, close to the theoretical Nernstian value of −59.2 mV/pH at room temperature (25 °C) for a reversible two-electron, two-proton process (Bard and Faulkner, 2001).

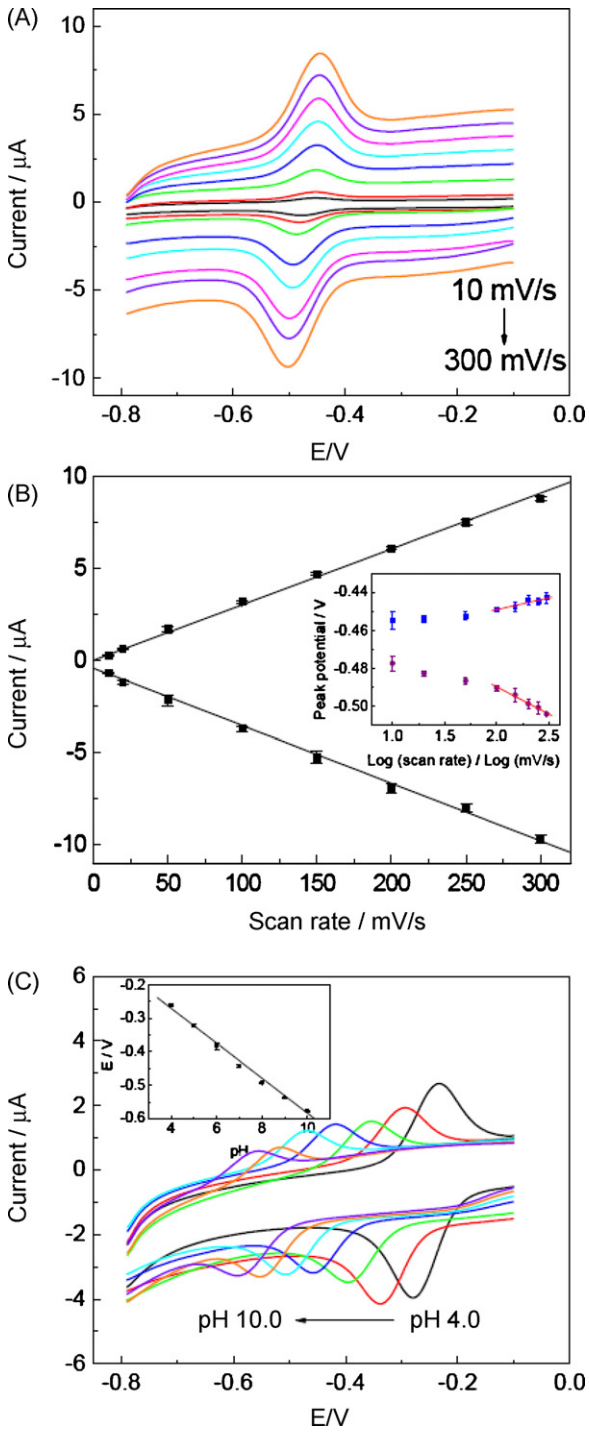

Fig. 3. (A) CVs of the pCoTTP-SWNTs-Nafion-GOD/GCE in N$_2$-saturated 0.01 M pH 7.4 PBS buffer at the scan rates of 10, 20, 50, 100, 150, 200, 250 and 300 mV/s, respectively. (B) The plot of the peak current vs. scan rate; inset presents the relationship between the peak potential (E_p) and the natural logarithm of scan rate (ln ν). (C) CVs of the pCoTTP-SWNTs-Nafion-GOD/GCE in PBS buffer of pH values ranging from 4.0 to 10.0 (scan rates = 50 mV/s); inset presents the plot of the formal potential E vs. pH.

3.3. Electroreduction of O_2 at the modified electrodes

We recently have shown the electrocatalytic properties of pCoTTP/GCE with respect to the four-electron reduction of oxygen (Chen et al., 2010). If these properties could also retain in the pCoTTP-SWNTs-Nafion-GOD-modified electrodes, they could become the basis for a practical oxygen reduction-based glucose

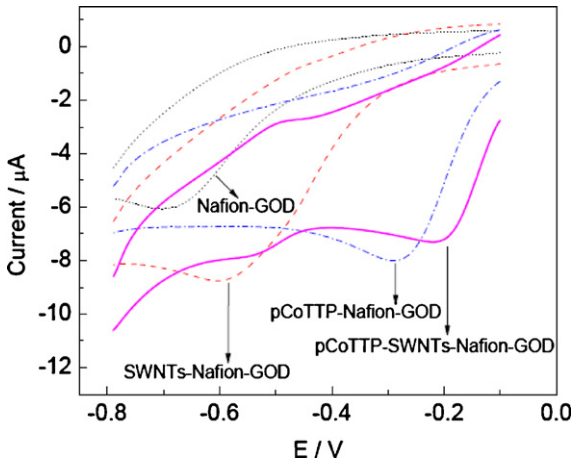

Fig. 4. CVs of the Nafion-GOD/GCE (dotted trace), SWNTs-Nafion-GOD/GCE (dashed trace), pCoTTP-Nafion-GOD/GCE (dashed-dotted trace), and pCoTTP-SWNTs-Nafion-GOD/GCE (solid trace) in air-saturated 0.01 M pH 7.4 PBS buffer (scan rates = 50 mV/s).

sensing. The remainder of this report will demonstrate its applicability.

Fig. 4 shows the electrocatalytic activities of the Nafion-GOD, SWNTs-Nafion-GOD, pCoTTP-Nafion-GOD and pCoTTP-SWNTs-Nafion-GOD-modified electrodes with respect to oxygen reduction. The oxygen reduction peak potential at the Nafion-GOD/GCE is at ca. −0.7 V slightly higher than the reported potential of −0.6 V at an unmodified GCE (Dai and Shiu, 2004). This can be rationalized by a retardation of the electron transfer between oxygen and the electrode surface that the Nafion-GOD layer may cause, resulting in a higher overpotential. Incorporating SWNTs into the electrode matrix (SWNTs-Nafion-GOD/GCE), the oxygen reduction peak potential shifts positively to −0.595 V, concomitant with an enhanced peak current. The SWNTs-induced peak potential shift at this electrode is ∼100 mV, indicating a much more facile oxygen reduction with a reduced overpotential. This improvement may be attributed to both enhanced electron transfer behavior and enlarged electroactive surface provided by SWNTs (Britto et al., 1999). Upon closer inspection of the CV trace for SWNTs-Nafion-GOD/GCE, an ill-defined redox peaks for GOD can be observed that is, however, overwhelmed by the oxygen reduction peaks. Furthermore, the pCoTTP-Nafion-GOD/GCE shows a largely improved catalytic property for oxygen reduction with a peak potential of −0.289 V. This is a reflection of the pronounced catalytic activity of the pCoTTP layer with respect to oxygen reduction (Chen et al., 2010). At the pCoTTP-SWNTs-Nafion-GOD/GCE, the oxygen reduction peak potential is further shifted positively to ca. −0.2 V, suggestive of a synergetic effect between the SWNTs and the pCoTTP-modified electrode surface. In addition, the CV at the pCoTTP-SWNTs-Nafion-GOD/GCE indicates that the activity of GOD is well preserved as the redox peaks from the direct electrochemistry of GOD are clearly present and, most significantly, the redox couple is well separated from the oxygen reduction peak region. These results clearly differentiate the electrode behavior of the pCoTTP-SWNTs-Nafion-GOD/GCE from that of all other electrodes discussed above and also indicates that the pCoTTP-SWNTs-Nafion-GOD/GCE provides enhanced electrocatalytic activity to oxygen reduction while being, at the same time, an excellent matrix for GOD immobilization.

3.4. Electrocatalytic properties of the modified electrodes towards glucose detection

The electrocatalytic properties of the modified electrodes towards glucose detection were first investigated by CVs. The

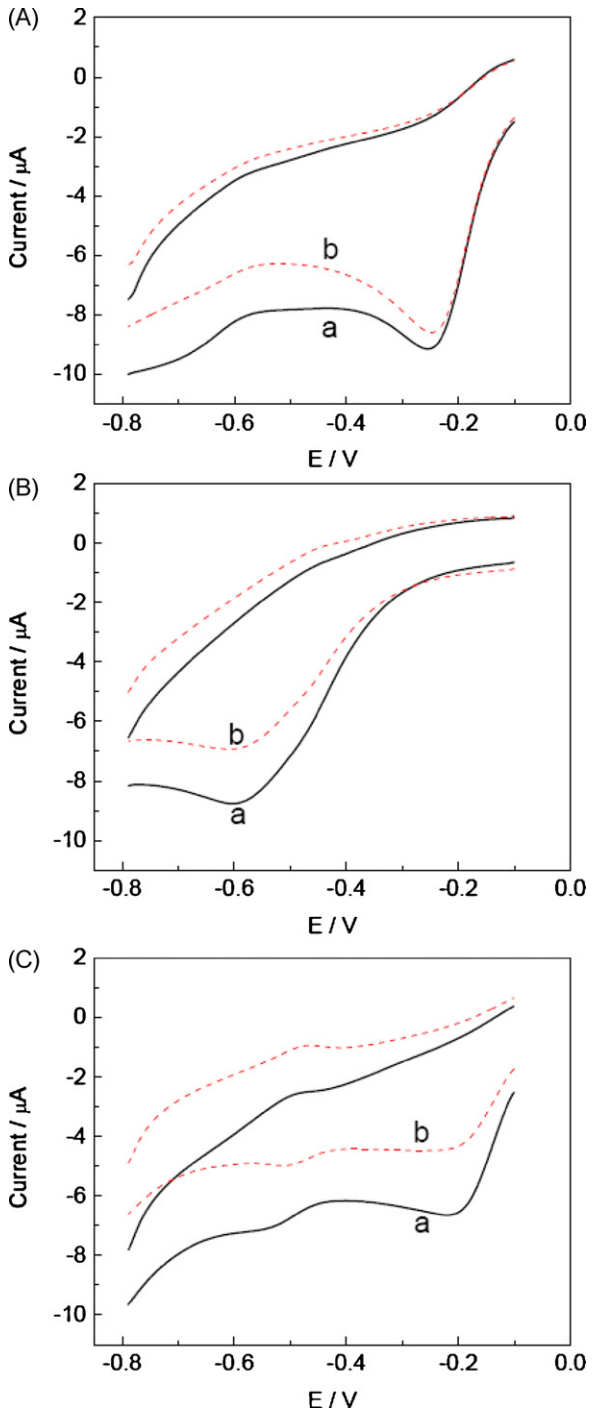

Fig. 5. CVs of the pCoTTP-Nafion-GOD/GCE (A), the SWNTs-Nafion-GOD/GCE (B), and the pCoTTP-SWNTs-Nafion-GOD/GCE in air-saturated 0.01 M pH 7.4 PBS buffer in the absence of glucose (a) and presence of 10 mM glucose (b) (scan rates = 50 mV/s).

responses to the presence and absence of 10 mM glucose at the three modified electrodes (pCoTTP-Nafion-GOD/GCE, SWNTs-Nafion-GOD/GCE, and pCoTTP-SWNTs-Nafion-GOD/GCE) were recorded in air-saturated 0.01 M pH 7.4 PBS buffer solution (Fig. 5). The oxygen reduction traces at all three modified electrodes show decreasing trends upon addition of glucose, reflecting the fact that GOD consumes oxygen when catalyzing the glucose oxidation (cf. Supplemental Fig. 1). However, different electrodes display different peak potential and peak current responses. The pCoTTP-SWNTs-Nafion-GOD/GCE exhibits the best performance in terms

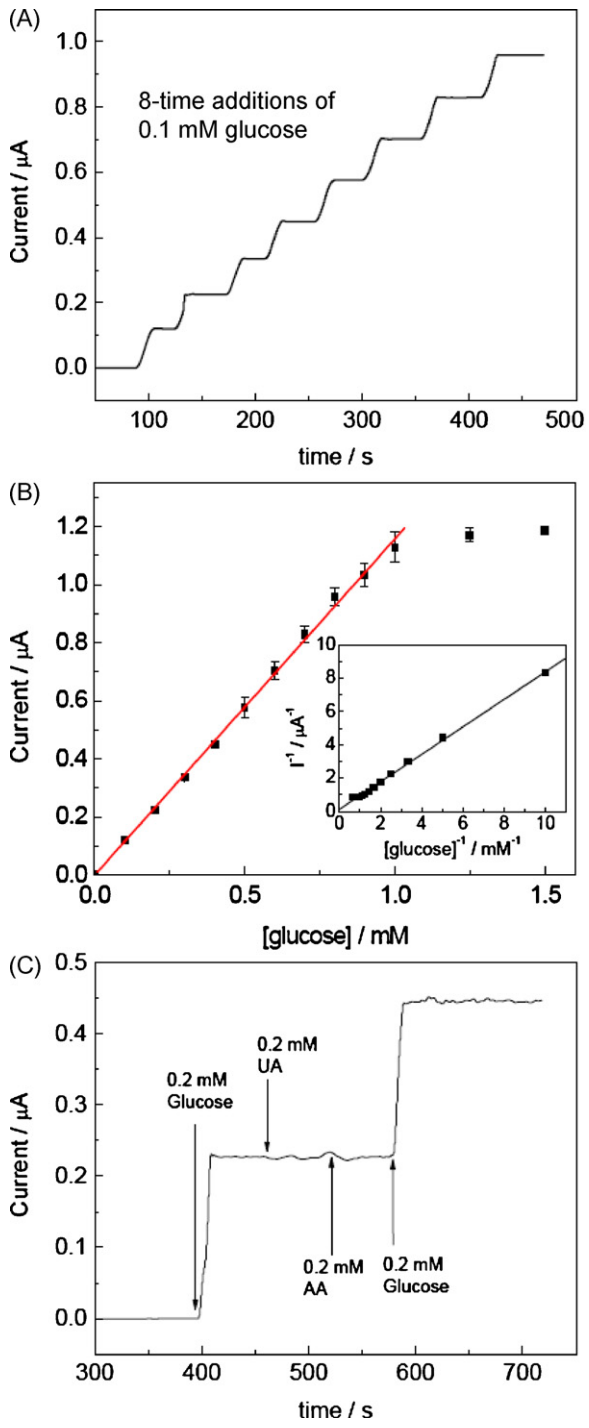

Fig. 6. (A) Amperometric response to successive addition of 0.1 mM glucose at the pCoTTP-SWNTs-Nafion-GOD/GCE after subtracting the baseline. (B) Calibration plot for glucose in air-saturated 0.01 M pH 7.4 PBS buffer at an applied potential of −0.2 V vs. Ag/AgCl. Inset presents the Lineweaver–Burk plot. (C) Amperometric response of the pCoTTP-SWNTs-Nafion-GOD/GCE to 0.2 mM glucose, 0.2 mM UA, 0.2 mM AA and 0.2 mM glucose, respectively, after subtracting the baseline.

of oxygen reduction peak potential and the reduction peak current change (Fig. 5C) when compared to the corresponding electrodes without SWNTs or pCoTTP. These results further indicate the existence of a synergetic effect between SWNTs and pCoTTP that can be utilized for oxygen reduction-based glucose detection.

Based on the CV results shown in Fig. 5, amperometric glucose detection was carried out in an air-saturated 0.01 M pH 7.4 PBS solution at an applied potential of −0.2 V (peak potential of oxygen reduction at the pCoTTP-SWNTs-Nafion-GOD/GCE) with continuous stirring. This applied potential is the lowest among recently reported oxygen reduction-based amperometric glucose biosensors (Bao et al., 2008; Noorbakhsh et al., 2008; Salimi et al., 2009; Wu et al., 2007, 2009). Such low applied potential is most important in GOD-based biosensors as it reduces possible interferences, resulting in highly selective responses to glucose (Lim et al., 2005; Pandey et al., 2003; Yu et al., 2003a). Fig. 6A shows typical amperometric responses of the pCoTTP-SWNTs-Nafion-GOD/GCE to the successive addition of 0.1 mM glucose after subtraction of the baseline. The modified electrode responds rapidly to the changes in glucose concentration, producing steady-state currents within 15 s after each addition. The calibration curve presented in Fig. 6B shows a linear range up to 1 mM (R^2 = 0.998) with a sensitivity of 16.57 μA mM^{-1} cm^{-2} and a detection limit of 5.33 μM (S/N = 3). Oxygen reduction-based glucose biosensors always show a narrow linear range (Bao et al., 2008; Noorbakhsh et al., 2008; Salimi et al., 2009; Wu et al., 2007, 2009) because of the fact that the low dissolved oxygen concentration in aqueous solution and fast oxygen consumption through enzymatic reaction result in saturated response at relatively low glucose concentrations.

The apparent Michaelis–Menten constant ($K_{m,app}$), which is an indicator of the affinity between the enzyme and substrate, can be derived from the modified Lineweaver–Burk equation $1/I_{SS} = (K_{m,app}/I_{max})(1/C) + (1/I_{max})$, where I_{ss} is the steady-state current after the addition of substrate, C is the bulk concentration of the substrate, and I_{max} is the maximum current measured under saturated substrate conditions. The smaller K_m value represents a higher enzyme affinity for glucose (Tan et al., 2005). From the Lineweaver–Burk plot (inset of Fig. 6B), the $K_{m,app}$ value of the glucose sensor was determined to be 0.98 mM. This value is as good as, or significantly better than the affinities recorded for cellulose/MWCNT/GOD-modified (1.1 mM) (Wu et al., 2009) and a MWCNT/Celestine blue/sol-gel/GOD-modified electrodes (2.4 mM) (Noorbakhsh et al., 2008).

Electroactive compounds such as uric acid (UA) or ascorbic acid (AA) present in serum samples frequently interfere with the electrochemical glucose sensors. Fig. 6C shows the amperometric response of the glucose sensor upon addition of glucose and, subsequently, 0.2 mM UA and 0.2 mM AA, followed again by glucose. It can be seen that the interferences from 0.2 mM UA and 0.2 mM AA are not observed and the sensor response to 0.2 mM glucose was also not affected by the addition of UA and AA. The excellent selectivity of the as-prepared glucose biosensor can be attributed to two factors: primarily, the low applied voltage required for glucose sensing is too low to oxidize either UA or AA (Reitz et al., 2008). Secondarily, the negatively charged Nafion film may also play certain role in eliminating the interferences by anions (Wang and Li, 1989).

4. Conclusions

The results suggest that pCoTTP-SWNTs-Nafion is an excellent matrix for GOD immobilization as it promotes the direct electron transfer to a very high degree, whereby both the nanodendritic pCoTTP and the SWNTs act cooperatively to assist in mediating the redox process. There is also a noticeable synergetic effect between the nanodendritic pCoTTP and SWNTs in the oxygen reduction reaction, shifting the oxygen reduction peak potential down to ca. −0.2 V. This allows the measurement of the oxygen reduction in the presence of GOD, laying the basis for the amperometric detection of glucose based on oxygen reduction. The apparent Michaelis–Menten constant ($K_{m,app}$) suggests a very good enzyme–substrate affinity. Thus, the developed pCoTTP-SWNTs-Nafion-GOD-based glucose biosensor exhibits very good

sensitivity. In addition, the biosensor exhibits excellent selectivity, as neither UA nor AA interferes with glucose sensing. In conclusion, the pCoTTP-SWNTs-Nafion-GOD/GCE biosensor represents a practical approach towards the development of highly sensitive and selective electrochemical glucose sensors based on oxygen reduction.

Acknowledgements

We greatly appreciate the partial support of this work by the US National Science Foundation under Grant No CMMI-0517782 (to YL and CB) and CHE-0517782 (to CB). We also thank the partial support from Science and Technology Directorate of the U.S. Department of Homeland Security. "Points of view in this document are those of the author(s) and do not necessarily represent the official position of the funding agencies."

Appendix A. Supplementary data

Supplementary data associated with this article can be found, in the online version, at doi:10.1016/j.bios.2010.07.062.

References

Azamian, B.R., Davis, J.J., Coleman, K.S., Bagshaw, C.B., Green, M.L.H., 2002. J. Am. Chem. Soc. 124, 12664–12665.
Bao, S.J., Li, C.M., Zang, J.F., Cui, X.Q., Qiao, Y., Guo, J., 2008. Adv. Funct. Mater. 18, 591–599.
Bard, A.J., Faulkner, L.R., 2001. Electrochemical Methods: Fundamentals and Applications. John Wiley & Sons, New York.
Britto, P.J., Santhanam, K.S.V., Ajayan, P.M., 1996. Bioelectrochem. Bioenerg. 41, 121–125.
Britto, P.J., Santhanam, K.S.V., Rubio, A., Alonso, J.A., Ajayan, P.M., 1999. Adv. Mater. 11, 154–157.
Cai, C.X., Chen, J., 2004. Anal. Biochem. 332, 75–83.
Chen, W., Akhigbe, J., Brückner, C., Li, C.M., Lei, Y., 2010. J. Phys. Chem. C 114, 8633–8638.
Courjean, O., Gao, F., Mano, N., 2009. Angew. Chem. Int. Ed. 48, 5897–5899.
Dai, Y.Q., Shiu, K.K., 2004. Electroanalysis 16, 1697–1703.
Demin, S., Hall, E.A.H., 2009. Bioelectrochemistry 76, 19–27.
Deng, C.Y., Chen, J.H., Chen, X.L., Mao, C.H., Nie, L.H., Yao, S.Z., 2008. Biosens. Bioelectron. 23, 1272–1277.
Ding, Y., Wang, Y., Li, B., Lei, Y., 2010. Biosens. Bioelectron. 25, 2009–2015.
Hecht, H.J., Kalisz, H.M., Hendle, J., Schmid, R.D., Schomburg, D., 1993. J. Mol. Biol. 229, 153–172.
Ivnitski, D., Artyushkova, K., Rincon, R.A., Atanassov, P., Luckarift, H.R., Johnson, G.R., 2008. Small 4, 357–364.
Jiang, L., McNeil, C.J., Cooper, J.M., 1995. J. Chem. Soc., Chem. Commun. 12, 1293–1295.
Laviron, E., 1979. J. Electroanal. Chem. 101, 19–28.
Lim, S.H., Wei, J., Lin, J.Y., Li, Q.T., KuaYou, J., 2005. Biosens. Bioelectron. 20, 2341–2346.
Lin, Y.H., Lu, F., Tu, Y., Ren, Z.F., 2004. Nano Lett. 4, 191–195.
Liu, G.Z., Paddon-Row, M.N., Gooding, J.J., 2007a. Electrochem. Commun. 9, 2218–2223.
Liu, J.Q., Chou, A., Rahmat, W., Paddon-Row, M.N., Gooding, J.J., 2005a. Electroanalysis 17, 38–46.
Liu, J.Q., Paddon-Row, M.N., Gooding, J.J., 2004. J. Phys. Chem. B 108, 8460–8466.
Liu, Y., Liu, L., Dong, S.J., 2007b. Electroanalysis 19, 55–59.
Liu, Y., Wang, M.K., Zhao, F., Xu, Z.A., Dong, S.J., 2005b. Biosens. Bioelectron. 21, 984–988.
Luo, X.L., Killard, A.J., Smyth, M.R., 2006. Electroanalysis 18, 1131–1134.
Luong, J.H.T., Hrapovic, S., Wang, D., Bensebaa, F., Simard, B., 2004. Electroanalysis 16, 132–139.
Musameh, M., Wang, J., Merkoci, A., Lin, Y.H., 2002. Electrochem. Commun. 4, 743–746.
Noorbakhsh, A., Salimi, A., Sharifi, E., 2008. Electroanalysis 20, 1788–1797.
Pandey, P.C., Upadhyay, S., Shukla, N.K., Sharma, S., 2003. Biosens. Bioelectron. 18, 1257–1268.
Patolsky, F., Weizmann, Y., Willner, I., 2004. Angew. Chem. Int. Ed. 43, 2113–2117.
Reitz, E., Jia, W.Z., Gentile, M., Wang, Y., Lei, Y., 2008. Electroanalysis 20, 2482–2486.
Salimi, A., Kavosi, B., Hallaj, R., Babaei, A., 2009. Electroanalysis 21, 909–917.
Tan, X.C., Ll, M.J., Cai, P.X., Luo, L.J., Zou, X.Y., 2005. Anal. Biochem. 337, 111–120.
Wang, J., Li, R., 1989. Talanta 36, 279–284.
Wang, J., Musameh, M., Lin, Y.H., 2003. J. Am. Chem. Soc. 125, 2408–2409.
Wu, L., Zhang, X.J., Ju, H.X., 2007. Biosens. Bioelectron. 23, 479–484.
Wu, X.E., Zhao, F., Varcoe, J.R., Thumser, A.E., Avignone-Rossa, C., Slade, R.C.T., 2009. Bioelectrochemistry 77, 64–68.
Xiao, Y., Patolsky, F., Katz, E., Hainfeld, J.F., Willner, I., 2003. Science 299, 1877–1881.
Yu, J.H., Liu, S.Q., Ju, H.X., 2003a. Biosens. Bioelectron. 19, 401–409.
Yu, X., Chattopadhyay, D., Galeska, I., Papadimitrakopoulos, F., Rusling, J.F., 2003b. Electrochem. Commun. 5, 408–411.
Zhang, J., Feng, M., Tachikawa, H., 2007. Biosens. Bioelectron. 22, 3036–3041.
Zhao, S., Zhang, K., Bai, Y., Yang, W.W., Sun, C.Q., 2006. Bioelectrochemistry 69, 158–163.